Structural Role of PbO in Li$_2$O–PbO–B$_2$O$_3$ Glasses

Munia Ganguli and K. J. Rao[1]

Solid State and Structural Chemistry Unit, Indian Institute of Science, Bangalore 560 012, India

Thermal and spectroscopic studies have been carried out on a number of glasses with wide ranging compositions in the pseudoternary glass system Li$_2$O–PbO–B$_2$O$_3$ in order to understand the structural role of PbO in these glasses. Infrared, Raman, and ^{11}B MAS-NMR results indicate that PbO behaves as a network former in these glasses and is possibly incorporated in the network as [PbO$_{4/2}$]$^{2-}$ units. The formation of [PbO$_{4/2}$]$^{2-}$ units leads to the creation of neutral three-coordinated boron (B$_3^0$) which, in turn, leads to the reformation of four-coordinated boron (B$_4^-$) in the structure at the expense of two-coordinated (B$_2^-$) and singly coordinated (B$_1^{2-}$) boron atoms. The variations of glass transition temperatures (T_g) and molar volumes also support this model.   © 1999 Academic Press

Key Words: lead glasses; glass spectra; structural role of lead.

INTRODUCTION

There is a renewed interest in the investigation of glasses which have potential as electrolytes for lithium batteries (1–6). Several strategies have been used to design novel lithium ion conducting glasses. Glasses with covalent networks often tend to possess open structures and support high ionic conductivities. The investigation of the structures of such materials is essential in order to give a better insight into structure–property relations. Lithium borates form good glasses over a wide range of compositions (7, 8). Boron atoms in these glasses are both three, and four-coordinated (9–17) and are generally designated as B$_3$ and B$_4$ units. B$_4$ units give rise to tetrahedral network features of the glass. The B$_4$/B$_3$ ratio is determined by the concentration of the modifier lithium oxide (9, 15, 18) but is also influenced by other constituents of the glass. A variety of anionic borate species such as penta-, tetra-, tri-, di-, pyro-, and orthoborates besides structural entities like boroxol rings with intermediate range order have been identified in modified borate glasses (16, 17). The concentration of the various borate species in the glass structure is determined by the nature and concentration of modifier oxides. For example,

the addition of lithium oxide, unlike other alkali oxides, not only modifies the B–O–B bonds but breaks up the tightly organized diborate units (19).

Lead oxide (PbO) is unique in its influence on the structure of glasses (20–23). It was observed in earlier studies from this laboratory that when PbO is added to network forming oxide glasses, it acts both as a network modifier and as a network former depending upon its concentration in the glass (24, 25). Network incorporated PbO has been found to be four-coordinated (24, 25). Raman spectroscopic studies have been reported on binary and ternary lead borate glasses which have a bearing on the structure and suggest that PbO may get incorporated into the network in four-coordinated positions (26–28). Several properties of molybdophosphate and tungstophosphorate glasses have been found to result from the incorporation of PbO into the network (29). It would therefore be very interesting to examine borate glasses containing both Li$_2$O and PbO. Although B$_2$O$_3$ is more acidic than PbO and is expected to take up the oxide ions from Li$_2$O on priority for the modification of B–O–B bonds, at the metaborate limit of modification PbO appears to be more acidic (3) than metaborate units and should be able to reclaim oxygen ions from the latter. In view of this possibility, Li$_2$O–PbO–B$_2$O$_3$ glasses synthesized over a wide range of compositions have been studied in this paper. Efforts have been made to understand the structural role of PbO in lithium borate glasses because it also has a direct bearing on the transport of Li$^+$ ions in these systems. The studies provide further input required for the design of glassy solid electrolytes in general. Thermal studies, infrared (IR), and Raman spectroscopies, as well as ^{11}B high resolution magic angle spinning nuclear magnetic resonance (HRMAS-NMR) spectroscopy have been used for the present investigations.

EXPERIMENTAL

Glasses were prepared by the conventional melt quenching method. The starting materials, Li$_2$CO$_3$ (Qualigens), PbO, and H$_3$BO$_3$ (BDH laboratory reagent) (all of Analar grade), were taken in appropriate proportions and ground

---

[1] To whom correspondence should be addressed.

TABLE 1
Nominal Compositions of the Glasses Prepared in the $Li_2O-PbO-B_2O_3$ Glass System, along with Their Codes, Densities, and Molar Volumes

	Composition (mole fraction)			Density	Molar volume (V_m)	Crystalline molar volume (V_c)
Code	PbO	Li_2O	B_2O_3	gm/cc	cc	cc
LB1	0.0	0.50	0.50	2.29	21.72	21.64
LB2	0.10	0.45	0.45	2.97	22.59	21.76
LB3	0.20	0.40	0.40	3.55	23.79	21.94
LB4	0.30	0.35	0.35	4.03	25.26	22.13
P1	0.20	0.50	0.30	3.49	23.06	20.6
P2	0.20	0.40	0.40	3.55	23.79	21.94
P3	0.20	0.30	0.50	3.61	24.49	23.29
P4	0.20	0.20	0.60	3.66	25.24	24.63
B1	0.0	0.70	0.30	2.20	19.00	18.89
B2	0.10	0.60	0.30	2.90	21.08	19.74
B3	0.20	0.50	0.30	3.49	23.06	20.6
B4	0.30	0.40	0.30	3.98	25.08	21.46
L1	0.0	0.50	0.50	2.29	21.72	21.64
L2	0.05	0.50	0.45	2.62	21.92	21.33
L3	0.10	0.50	0.40	2.94	22.15	21.09
L4	0.15	0.50	0.35	3.24	22.47	20.84
L5	0.20	0.50	0.30	3.49	23.06	20.6
L6	0.25	0.50	0.25	3.70	23.82	20.36

together to constitute a 5–10 gm batch. The ground mixtures were heated in porcelain crucibles at ≈ 650 K for about 4–5 hours in a muffle furnace. The batches were then melted at 1225 K for about 10 min, stirred to ensure homogeneity, and quenched between stainless steel plates kept at room temperature. The nominal compositions of the glasses prepared along with their codes are listed in Table 1. In order to confirm that there was negligible loss of PbO and Li_2O during melting, we weighed the initial reaction mixture and the final products for some of the compositions. The loss was indeed found to be negligible. For example, for the composition LB4, the weight loss of 5.0 gm of sample was found to be 0.0073 gm. Assuming that only the loss of PbO was responsible for this, the final composition was estimated to be $0.299PbO-0.3505Li_2O-0.3505B_2O_3$, which is negligibly different from the nominal composition. Hence, we did not make any further attempts toward estimation of the compositions. The glasses prepared have been grouped into four categories and in each category, the proportion of one or a combination of two components is held constant. For example in the L series the percentage of Li_2O is held constant whereas in the LB series Li_2O/B_2O_3 (lithium borate) is held constant. Since some of the compositions are such that they belong to two groups they find duplicate entries in different categories in Table 1. The glasses were all transparent and mostly colorless though some of the compositions rich in PbO were pale yellow in color.

The amorphous nature of the samples was confirmed using powder X-ray diffraction (JEOL JOX-8P X-ray diffractometer). The glass transition temperatures (T_g) and heat capacities (C_p) were determined using a differential scanning calorimeter (Perkin Elmer DSC 2). Dry nitrogen was used as a purge gas. For specific heat measurements, glass wafers weighing about 20–30 mg were taken in gold pans. The samples were first annealed at temperatures about 20 K below T_g (a rough estimate of T_g itself was obtained from a prior 20 K/min scan) and DSC scans for C_p measurements were carried out at a uniform heating rate of 10 K/min. Single crystalline alumina (sapphire) was used as the calibration standard for calculating C_p. The accuracy of the measured C_p values was found to be about 2%. T_g values were determined by extrapolating the linear portions around the glass transition region in the C_p vs T plots.

Densities (ρ) of annealed glass bits free of air bubbles and cracks (determined by visual examination) were measured by the standard Archimedean (apparent weight loss) method using xylene. The weights of the glass bits were about 0.3 to 1 gm. The molar volume of each composition was calculated as $V_m = M/\rho$, where M is the molecular (formula) weight of the glass. The accuracy of the measured density values was found to be about 0.05%.

IR transmission measurements were made of KBr pellets over the range of 4000 to 400 cm^{-1} using a Nicolet 740 FTIR spectrometer. Unpolarized Raman spectra were recorded (in the range of 100 to 1500 cm^{-1}) on a SPEX 1403 Raman spectrometer making use of the excitation wavelength of 514.5 nm from an Argon–ion laser. Glass pieces of approximately 1 cm^2 area and 0.8 to 1 mm thickness were used for the Raman measurements.

^{11}B HRMAS-NMR spectra of powdered glass samples were recorded using a Bruker DXL 300 solid state high resolution spectrometer (magnetic field = 7.05 Tesla) operating at 96.4 MHz. 90° pulses of 5 μs duration were employed with a delay of 10 seconds between the pulses. A cylindrical zirconia rotor was used to spin the samples with speeds of 3–7 KHz. The spinning sidebands were identified by virtue of their drifts when samples were spun at different speeds. The chemical shift values were measured with respect to $(CH_3)_3B$.

RESULTS AND DISCUSSION

Molar Volumes

The densities and molar volumes (V_m) of all the glasses prepared are listed in Table 1. The sum of the molar volumes of the components of the glass in their crystalline states ($V_c = \sum V_i$, where i represents the ith component of the glass) have also been calculated and listed in the table. The glass molar volumes are greater than the crystalline molar volumes in all the compositions indicating more open structures in the glass than in the hypothetical mixed

crystalline phase of the same composition. It also indicates the presence of excess structural volume in the glass. Among all the glasses in Table 1, a maximum increase in molar volume is observed in the B series where the concentration of PbO is increased at the expense of Li_2O (a corresponding decrease occurs in the Li_2O/B_2O_3 ratio). The increase in molar volumes is not as high when the Li_2O/B_2O_3 ratio is held constant, as in the LB series or when the ratio is increased with a simultaneous increase in PbO content, as in the L series. There is an increase in molar volume when the PbO concentration is held constant and the Li_2O/B_2O_3 ratio is decreased, as in the P series of glasses. Alternatively expressed, there is a decrease in the molar volumes of the glasses in P series as the Li_2O/B_2O_3 ratio increases. In fact in the highly modified regime in this series which contains discrete borate ions, the constituents seem to fill space more efficiently, which also brings about a decrease in the differences between V_m and V_c as seen in Table 1. Down the LB series the differences between V_m and V_c increase, suggesting that the addition of PbO has the effect of increasing the molar volume. If the glasses in the pseudobinary $LiBO_2$–PbO (LB) series were to be an ideal mixture, the expected volumes of the glasses would be weighted linear sums of the volumes of glassy $LiBO_2$ and PbO. Since the molar volume of glassy $LiBO_2$ is known (corresponding to that of LB1), the molar volume of glassy PbO itself can be calculated on the basis of this assumption: $V_m = xV_{LiBO_2} + (1 - x)V_{PbO}$, where x is the mole fraction of $LiBO_2$ present in the glass. The molar volume of glassy PbO is expected to be a constant. But the calculated molar volumes of glassy PbO are equal to 30.42, 32.07, and 33.52 cc for the glasses LB2, LB3, and LB4, respectively, and the values indicate a systematic increase with increasing concentration of PbO in the glass. Thus the contribution of PbO to glass molar volumes increases nonlinearly with its concentration. This observation indicates incorporation of PbO and a consequent reversal of the modification of B_2O_3 itself. This aspect will be discussed later, but it suggests that PbO is incorporated into the network as $[PbO_{4/2}]^{2-}$ ($=P_4^{2-}$) units (29).

Such a nonlinear increase in volume might not have been possible if PbO behaved as a modifier because the metaborate network would have been further degraded and the resulting (chain terminating) pyroborate units would have led to more efficient packing, causing the molar volumes to decrease. Therefore, we should expect that an increase in PbO would bring about an effective increase in the molar volume of the glass by its tendency to behave like a network former.

The different types of borate and plumbate (lead oxide) structural units that are likely to be present in these glasses are listed in Table 2 along with their designation as used in the text. It may be noted that if PbO were to enter the network (along with the borate) as $[PbO_{4/2}]^{2-}$, it would

TABLE 2
Different Structural Units Present in Li₂O–PbO–B₂O₃ Glasses along with Their Notations

Structural unit	Notation
$[BO_{3/2}]^0$	B_3^0
$[BO_{2/2}O]^-$	B_2^-
$[BO_{1/2}O_2]^-$	B_1^{2-}
$[BO_{4/2}]^-$	B_4^-
$[PbO_{2/2}]^0$	P_2^0
$[PbO_{4/2}]^{2-}$	P_4^{2-}

have to compete with B_2O_3 for the oxygen available from the modifier Li_2O, since PbO is identically $[PbO_{2/2}]^0$, and a reaction of the type

$$[PbO_{2/2}]^0 + O^{2-} = [PbO_{4/2}]^{2-}$$
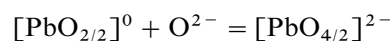
should take place. Thus, the addition of PbO can be considered as taking away O^{2-} ions from the modified borate network and reconverting metaborate B_2^- units into neutral B_3^0 units in the network. The conversion would not only affect the chemistry of the borate part of the network would also affect the B_3–B_4 (or more appropriately B_3^0–B_4^-) equilibrium as discussed later. Formation of B_3^0 at the expense of B_2^- can also be expected to increase the molar volume as it reconstitutes the more open network of a less modified glass.

The molar volumes of glasses in the B series are remarkably high because in this series PbO is increased and the concentration of the modifier Li_2O is decreased. Both of these factors contribute to increase volumes; because a decrease of modification of borate regenerates B_3^0 units (also B_2^- from B_1^{2-}) and an increase in PbO gives rise to network forming P_4^{2-} type units. In the L series of glasses, one should expect the modification by Li_2O to be more pronounced as we go down the series (L1 to L6) and therefore a decrease in the molar volumes. On the contrary, there is a clear increase in the volume which is possible only if PbO plays the role of a network former, whereupon the extent of modification of B_2O_3 is effectively reduced and the network is extended by the formation of P_4^{2-} units. Thus the molar volume variation in all the four series of glasses are strong indications of a network forming role of PbO.

Thermal Properties

The glass transition temperatures (T_g) of the various glasses, the heat capacities at ($T_g - 20$)K, and the Dulong Petit heat capacities are listed in Table 3. The values of T_g span a wide range of temperatures (570 and 690 K) and show discernible systematics in their variation as a function of composition. There seem to be two factors which

TABLE 3
Thermal Properties of the Li_2O–PbO–B_2O_3 Glasses

Sample	T_g K	C_p (at $T_g - 20K$) $JK^{-1} mol^{-1}$	$3nR$ $JK^{-1} mol^{-1}$
LB1	690	98.9	99.8
LB2	638	85.9	94.8
LB3	625	72.5	89.8
LB4	612	60.2	84.8
P1	595	76.2	84.8
P2	625	72.5	89.8
P3	660	84.0	94.8
P4	700	88.1	99.8
B1	585	83.0	89.8
B2	570	76.2	87.3
B3	595	76.2	83.3
B4	620	70.0	82.3
L1	690	98.9	99.8
L2	628	84.2	96
L3	623	71.9	92.3
L4	603	77.0	88.5
L5	595	76.2	84.8
L6	600	75.9	81.1

influence the variations of T_g: the PbO content and the Li_2O/B_2O_3 ratio. T_g decreases with an increase in both these factors, as manifested very clearly in the T_g values of the four series of glasses. The dependence of T_g arises because an increase in PbO results in the formation of a weakened network consisting of $[PbO_{4/2}]^{2-}$ units and the T_g decreases. Also the increase of the Li_2O/B_2O_3 ratio breaks up the network, making the glass more ionic, which generally decreases the T_g (30). Keeping Li_2O/B_2O_3 a constant and increasing PbO (see LB series) also results in a drop in T_g. This is clearly consistent with the proposed consequences of increasing PbO. Holding the concentration of PbO constant and decreasing the Li_2O/B_2O_3 ratio results in an increase in T_g as seen in the P series. This is consistent with the restoration of the stronger B_3–B_4 network. When Li_2O/B_2O_3 and PbO are varied in opposite manners, as in the B series, the range of variation in T_g values is reduced significantly. However, a shallow minimum occurs in T_g variation which is a resultant of the opposing influences of increasing PbO and decreasing the Li_2O/B_2O_3 ratio. This is again consistent with the role of PbO and the effect of modification. As noted in the earlier section, the formation of P_4^{2-} can occur only at the expense of B_2^- or a B_4^- which is converted to B_3^0. Thus the network features generally increase with either an increasing concentration of PbO or a decreasing Li_2O/B_2O_3 ratio. The magnitude of the effect of increasing PbO which contributes to the formation of a weaker network appears to be lower than the magnitude of the effect of altering the Li_2O/B_2O_3 ratio, as seen in the T_g variation in the P series.

The glass transition temperatures of P4 and LB1 are very similar. While LB1 is a pure metaborate glass, P4 is a glass of ultraborate composition with 20% PbO. The average spatial dimensionality of the network in P4 must be greater than 2 (assuming the dimensionality of P_4^{2-} and B_4^- as 3, of B_3^0 as 2, and of B_2^- as 1), while that of LB1 should be close to unity because the concentration of B_4^- centers in metaborate is low (15). It is indeed low because in its stable configuration, a B_4^- is always separated from other B_4^- units by intervening B_3^0 units as in a diborate glass. Two B_4^- units are never found to be directly connected in the glass structure. In metaborate composition a B_4^- is necessarily separated from the other B_4^- units by intervening B_2^- units, thus setting an upper limit of 33.3% for the B_4^- concentration. The observed values are generally lower. Since the T_g of P4, which has higher spatial dimensionality, is similar to that of LB1, which has a lower spatial dimensionality, the view is supported by the fact that the bonds in P_4^{2-} are much weaker than the bonds in either B_3^0 or B_4^- units.

The heat capacities of all glasses are considerably lower than the Dulong Petit heat capacities. The glass transition behavior was found to be generally sharp and the variation of C_p was almost step-like in all cases. There was also clear evidence of relaxational humps in the heat capacity plots. Large differences between the Dulong Petit and observed heat capacities are generally indicative of the fact that vibrational modes are not all fully excited below T_g. The variation of the heat capacity differences is very remarkable in the LB series. In the pure metaborate glass (LB1), the heat capacity difference is negligible and T_g is also the highest. But as PbO is introduced, the heat capacity differences increase suggesting that in PbO-rich glasses, the T_g values being lower, the temperatures may not be sufficient for the excitation of all the vibrational modes. However, there is a component of the observed differences in heat capacities which arises from frozen entropies. The magnitude of the frozen entropy is dependent upon the temperature dependence of melt viscosities just above T_g. Since PbO-rich glasses may arguably possess higher spatial dimensionalities, their viscosities above T_g and hence the frozen entropies in them may be higher. This evidently contributes to the manifestation of a greater difference in heat capacities in PbO-rich glasses as observed in Table 3.

Infrared Spectra

The infrared spectra of these glasses arise largely from the modified borate network. The IR absorptions of borate glasses occur in two regions, those between 1200 and 1400 cm^{-1} which arise from borate units in which boron atom is connected to three oxygens (both bridging and nonbridging types) such as B_3^0 and B_2^-, etc and those between 900 and 1100 cm^{-1} due to boron in a tetrahedral oxygen coordination (B_4^-) (19, 31–33). B–O–B bending

vibrations manifest themselves in the lower frequency region of 600–800 cm^{-1} in the IR spectra (31–33). It is seen from Fig. 1a that the spectral of LB1, which is a pure metaborate, has strong absorptions corresponding to both B$_3$ (1425 and 1252 cm^{-1}) and B$_4$ (1027 cm^{-1}). The realtive intensities of these peaks also undergo significant changes as the PbO content increases. The trigonal boron peak at 1435 cm^{-1} is significantly red-shifted as the PbO content increases. Since the B$_4$ concentration is expected to be low in metaborates, high intensities of the peaks corresponding to B$_4$ may be a consequence of larger values of $\Delta\mu/\Delta r$ where μ is the transition dipole moment, r is the corresponding coordinate for the bond stretching mode which brings about a redistribution of charges, and Δ represents the change in these quantities during the transition (34). Since the tetrahedrally connected B$_4^-$ species has an even distribution of negative charge, redistribution of its charge during a vibrational transition may be more readily achieved than in a B$_2^-$ species in which the bond asymmetry is high. The IR absorption due to trigonal borons is red shifted and its intensity becomes significantly higher. But even more interestingly, absorption due to B$_4$ also increases, significantly down the series (LB1 to LB4). In order to understand this behavior we recall that the B$_4^-$ units in the borate glasses are never connected to each other and that there is an inherent limit for the maximum concentration of B$_4^-$/B$_2^-$ in the glass is the ratio 2:4. Therefore, the 33.3% concentration of B$_4$ and its reasonably higher extinction coefficient can perhaps account for the comparable intensities of B$_3$ and B$_4^-$ in the spectrum of LB1. Since 33.3% B$_4$ is higher than the proportions reported experimentally for this glass (15, 35), we surmise that B$_4^-$ units connected to B$_2^-$ units in the structure are less stable than those connected to B$_3^0$ units. However, it is possible that B$_3^0$ can be present in the glass as it is produced by a disproportionation of B$_2^-$ units and some of the B$_4^-$ units in the structure are stabilized:

$$2B_2^- = B_3^0 + B_1^{2-}.$$

But more importantly, B$_3^0$ is created by the reaction of P$_2^0$ with B$_2^-$ and in the process P$_2^0$ converts itself to P$_4^{2-}$. This conversion involves some geometrical constraints because the Pb atom carries a lone pair and it is likely that the four-coordinated lead is present in a square–pyramidal geometry. We visualize the reaction as shown below:

$$[PbO_{2/2}]^0 + 2(B_2^-)_2 = [PbO_{4/2}]^{2-} + 2(B_3^0 B_2^-).$$
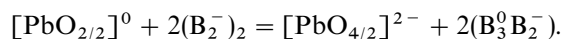
$(B_2^-)_2$ is identically
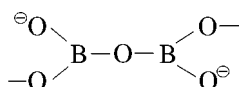
and is a binary bit of the metaborate chain and $(B_3^0 B_2^-)$ is
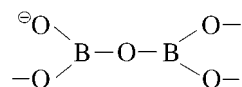
which results after the reaction. The above reaction seems quite feasible since the molecular electronegatives are 2.36, 1.96, 1.00, and 2.31, respectively, for the four species (calculated using Sanderson's procedure (36)). The electronegativities of the products lie between those of the reactants which is a satisfactory criterion for the reaction to occur (37). However, an isolated B$_2^-$–B$_3^0$ reduction may not be favored because isolated B$_3^0$ has a molecular electronegativity (2.71) which is greater than that of $[PbO_{2/2}]^0$ (2.36). Therefore, enough B$_3^0$ is created in the system which reconverts B$_2^-$ to B$_4^-$ and stabilizes them in the structure. Thus the concentrations of both B$_3^0$ and B$_4^-$ increase and the IR absorption due to both B$_3^0$ and B$_4^-$ intensify as seen in the spectra (Fig. 1a). The 1252 cm^{-1} absorption peak can be attributed to the symmetrical stretching of B$_3$ units and the increasing intensity of this band down the LB series is consistent with the above analysis.

The IR spectra of P1 to P4 reveals that the intensities corresponding to symmetrical and asymmetrical stretching of B$_3$ continues to rise in intensity down the series, but rather remarkable is the growth in intensity of the B$_4$ units. It is to be expected that P$_2^0$ = P$_4^{2-}$ conversion initially occurs through simultaneous conversions of B$_2^-$ to B$_3^0$ and also B$_1^{2-}$ to B$_2^-$. Since P1 is nearly a fully pyroborate composition, it is evident that the concentration of B$_3^0$ and hence B$_4^-$ is very low in P1. But as the Li$_2$O/B$_2$O$_3$ ratio decreases down the series, a significant increase in the concentration of B$_4^-$ occurs and is consistent with the spectra in Fig. 1b. The presence of higher concentrations of neutral B$_3^0$ entities may be responsible for the slight softening of the bending mode from 717 to 682 cm^{-1} down the series (P1 to P4).

The behavior of the IR spectra of the glasses in the B series is also consistent with the network forming role of PbO. In the PbO-free B1 composition which should have pyro and even orthoborate units there is hardly any evidence of B$_4^-$ units. There is a sharp B–O–B bending which should be expected of small pyroborate units and it also occurs at slightly higher frequencies due to increased intramolecular repulsions of charged oxygens in the pyroborate structure. With the increasing concentration of PbO, intensities due to B$_4^-$ units also increase in the region of 900–1100 cm^{-1}.

In the L series of glasses, the IR spectrum of L1 is the same as that of LB1 and was discussed earlier. When the PbO content is increased down the series (L1 to L6) there is evidently an increased production of B$_3^0$ units in the structure which is reflected in the enhanced symmetrical stretching in the region of 1250 cm^{-1}. However, we note here that
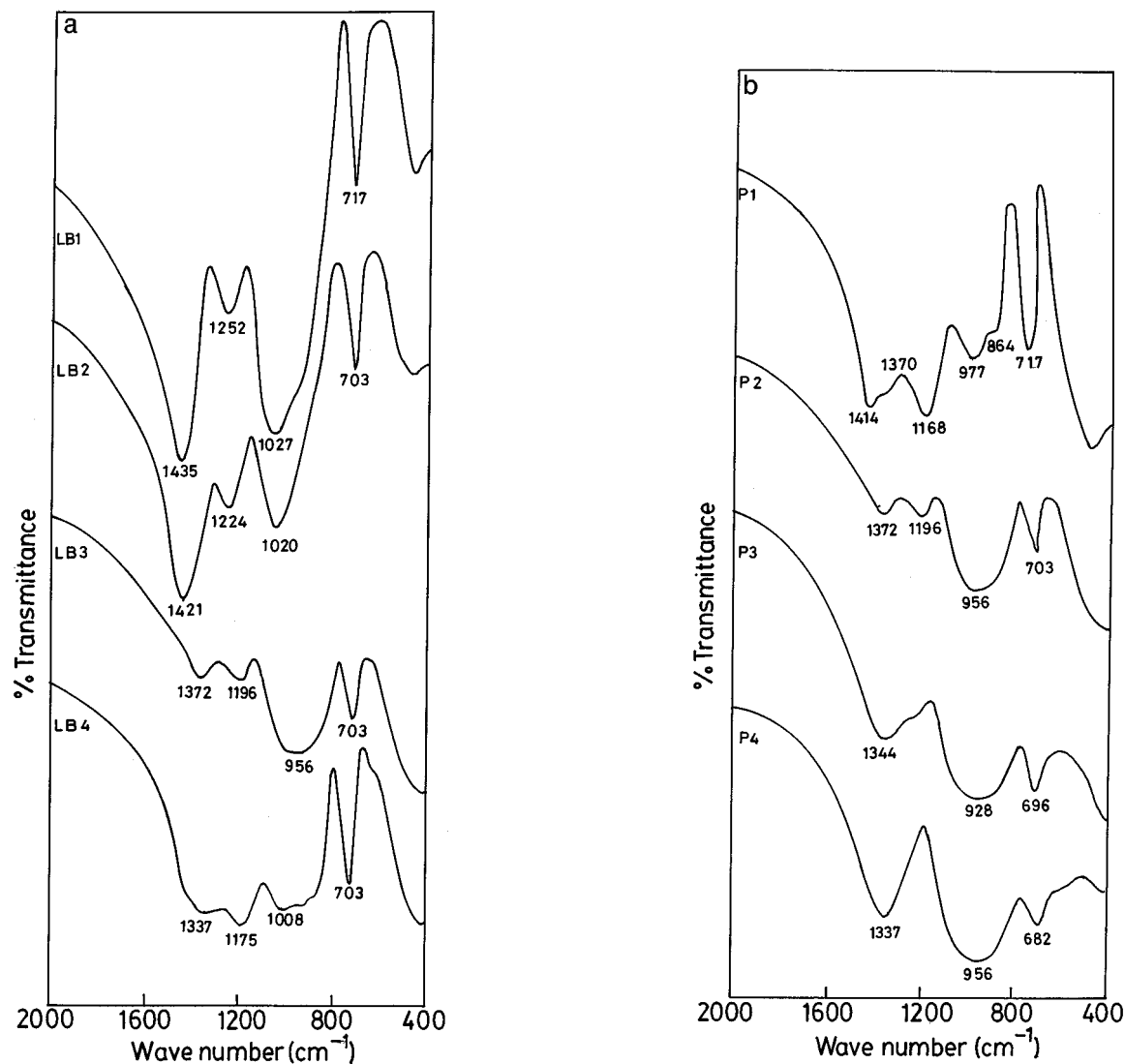
FIG. 1. Infra-red spectra of (a) constant Li_2O/B_2O_3 (LB) series, (b) constant PbO (P) series, (c) constant B_2O_3 (B) series, and (d) constant Li_2O (L) series in glass system Li_2O–PbO–B_2O_3.

the 1250 cm^{-1} peak is not present in pure alkali diborate glasses (37) in which the concentration of B_3^0 and B_4^- are expected to be equal and all B_3^0 units are presumably connected only to B_4^- units. In such a symmetrically connected B_3^0 unit the vibrational transition is likely to be symmetry forbidden. This is supported by the IR spectra of borovanadate glasses in which the 1250 cm^{-1} peak is seen and is attributed to vibrations in diborovandate species (37) and B_3^0 in the diborovandate species is indeed asymmetrically substituted. However, the 1250 cm^{-1} peak in the present glasses arises from the symmetrical stretching of B_3 units which are asymmetrically connected in the structure to other units such as a combination of P_4^{2-}, B_2^-. Therefore, the IR spectra of these glasses are consistent with the presence of a network structure formed by both PbO and B_2O_3.

Raman Spectra

The Raman spectra of the glasses are presented in Fig. 2. In the Raman spectrum of pure lithium metaborate glass LB1 in Fig. 2a, there is a broad peak around 1485 cm^{-1} and another at 967 cm^{-1} which are attributed to B_3^0 and B_4^- units (38–41). Most vibrational modes in B_2O_3 and borates are both IR and Raman active (42). The 765 cm^{-1} peak is attributed to the B–O–B bending mode (38–40). This band appears to get blue shifted and we feel that blue shifts can also be due to increased O$^-$–O$^-$ repulsion on adjacent borate groups. The 535 cm^{-1} peak is often assigned to diborate units (38–40) which, in the presence of PbO in LB2, LB3, and LB4, appears to be completely eliminated. The presence of diborate in LB1 can be rationalized only by
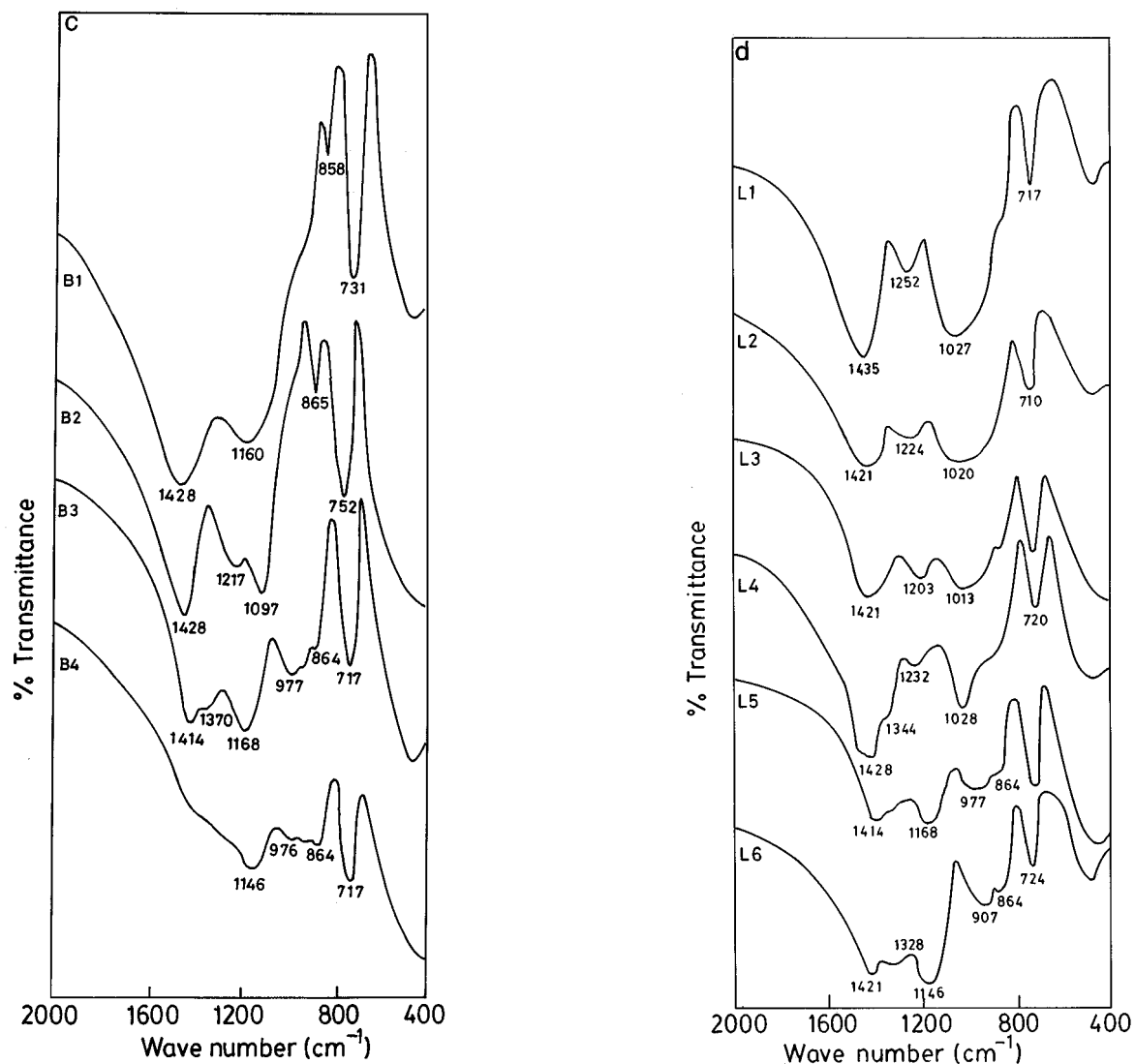
FIG. 1—*Continued*

invoking the disproportionation reaction of B$_2^-$ which was suggested earlier, B$_2^-$ = B$_3^0$ + B$_1^{2-}$, which generates B$_3^0$ required for the formation of diborate units. Notable features of the spectra of LB2, LB3, and LB4 are: the emergence of new peaks in the region of 280–300 cm^{-1} which we attribute to P$_4^{2-}$ units formed by the incorporation of PbO into the network and the emergence of peaks in the region of 1200 cm^{-1} due to symmetric stretching of B$_3$ units also generated during the incorporation of PbO into the structure. Correspondingly, the intensity of the peaks due to tetrahedral B$_4^-$ units also increases, reasons for which were discussed earlier. The new feature in the 640 cm^{-1} region may be attributed to a bending mode of the Pb–O–B links in the new structure.

The Raman spectra of the P series of glasses are also consistent with the incorporation of PbO into the network. There is a new peak at 290 cm^{-1} due to P$_4^{2-}$ which merges into a broad shoulder in P3 and P4. There is a large increase in the intensities of the peaks in the B$_3$ region (1200–1400 cm^{-1}). The intensity of the symmetrical mode at 1216 cm^{-1} decreases in the B$_2$O$_3$- rich compositions. As it is generally attributed to the symmetrical B$_3$ model it is likely that in B$_2$O$_3$ rich glasses (less modified) there is a decrease in asymmetrically connected borate units. The intensity of the Raman peaks due to B$_4^{-1}$ decreases expectedly in P3 and P4 because they are B$_2$O$_3$-rich (ultraborate) compositions. Since PbO (P$_2^0$) also makes a demand on the available B$_2^-$ units for connecting itself into P$_4^{2-}$, the
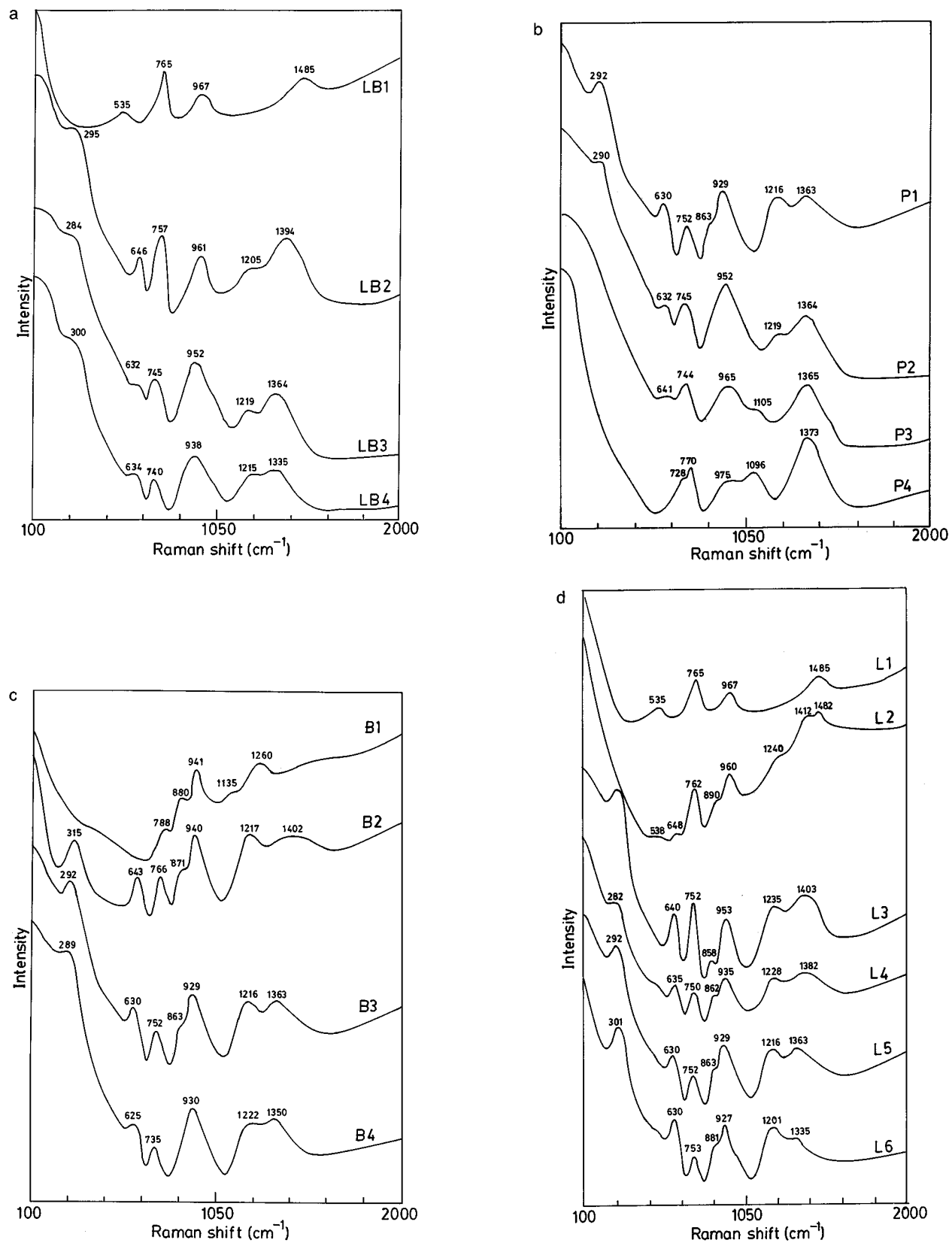
FIG. 2. Raman spectra of (a) constant Li_2O/B_2O_3 (LB) series, (b) constant PbO (P) series, (c) constant B_2O_3 (B) series, and (d) constant Li_2O (L) series in the glass system Li_2O–PbO–B_2O_3.

concentration of B$_3$ units increases further and correspondingly the concentration of B$_4$ units decreases. The bending mode of B–O–Pb links in the 630 cm^{-1} region appears to be slightly blue shifted and in P4 merged into the shoulder of the 770 cm^{-1} peak. The bending mode B–O–B in P4 appears to be split in these borate rich glasses. The Raman peak in the 1100 cm^{-1} region present in P3 and P4 may be due to the emergence of diborate units (38–40) in the borate-rich structures, which are also enriched in B$_3^0$ due to the presence of PbO.

Raman spectra of B1 exhibits 880 and 940 cm^{-1} features due to B$_4$ and the 1135 and 1260 cm^{-1} peaks due to trigonal boron. The B–O–B bending modes are evidently more energetic due to the presence of a highly modified pyroborate structure characterized by strong repulsions of O$^-$ ions on neighboring borons. B2, B3, and B4 glasses in which PbO is present in increasing concentrations give rise to Raman peaks at 643 (due to Pb–O–B bending) and 300 cm^{-1} (due to P4 units). Softening of the B–O–B bending vibration (766 to 735 cm^{-1}) down the series is due to the conversion of B$_2^-$ (and also in two successive steps B$_1^{2-}$) to B$_3^0$ and the emergence of the 1216 cm^{-1} peak is due to symmetric stretching of the B$_3$ units (symmetrically connected in less modified compositions).

In the L1 to L6 glasses we again witness the disappearance of the diborate peaks at 535 cm^{-1} as the PbO concentration increases down the series. The emergence of peaks at 280–300 cm^{-1} (due to P$_4^{2-}$) in L3 to L6, at 640 cm^{-1} (due to B–O–Pb bending), and at 1200–1240 cm^{-1} (due to B$_3$ vibrations which are asymmetrically connected) are all consistent with the incorporation of PbO into the network. Stretching modes of the B$_4$ units exhibit splitting down the series, indicating asymmetric connectivities. L4 to L6 glasses indicate the gradual emergence of a shoulder of nontrivial intensity around 430 cm^{-1} which may be due to Li$^+$ ion vibrations in the oxygen ion cages (43, 44). In general, the stretching frequencies of the trigonal borons (1200–1240 cm^{-1}) exhibit a decrease in frequency down the series which is an indication of increased (average) modification. Thus, the Raman spectra of the borate glasses are clearly consistent with the role of PbO as a network former.

^{11}B HR-MASNMR Spectra

^{11}B MASNMR spectra for all the samples are shown in Fig. 3. The spectra reveal the presence of a sharp resonance at around -17 ppm (with respect to the resonance signal of trimethyl boron (45)) which arises from the B$_4$ species (15, 18, 35, 37, 46–51). There is a split peak in the base of all the B$_4$ signals which arises from boron atoms in three-coordination (15, 18, 35, 37, 46–51). These three-coordinated boron atoms include B$_3^0$, B$_2^-$, and B$_1^{2-}$ as far as MASNMR is concerned because there is no further resolution of the signals arising from them in the spectra. Thus all

the spectra have the appearance of a B$_4^-$ resonance peak with wings at the base, as is expected in glasses containing boron atoms in two-coordinations. The area under the composite spectrum has been apportioned to B$_4$ ($=$ B$_4^-$) and B$_3$ ($=\sum$B$_i$, $i = 1$ to 3) present in the glass by connecting the peaks of the quadrupolar split B$_3$ with a smooth line. Such apportionment of the composite peaks due to B$_3$ and B$_4$ has been found to have little uncertainty and the trends in their variation are particularly reliable (35, 37, 46, 48). The values of N_4, where $N_4 = $ B$_4/$(B$_3 + $ B$_4$), have been calculated for all the glasses and are listed in Table 4.

The N_4 values have been plotted in Fig. 4 against y/z where y and z are the concentrations of Li$_2$O and B$_2$O$_3$, respectively. Also included in the plot of Fig. 4 are a few experimental points of N_4 in the binary Li$_2$O–B$_2$O$_3$, system known from the literature (35). It is well known that beyond the diborate composition ($y/z > 0.5$) N_4 decreases from its maximum value of 0.5 as a function of y/z (15, 35). We have found that the variation of N_4 in this region is represented reasonably well by the empirical function $1/2\exp(1/2-y/z)$ (52). Behavior of this function is shown in the plot as a dotted line. It may be seen that the values reported in the literature agree reasonably well with the empirical function. But the values of N_4 determined in the present work are considerably higher, particularly between $y/z = 1.0$ (metaborate) and $y/z = 2.0$ (pyroborate).

It may be noted that in $N_4 = $ B$_4/$(B$_3 + $ B$_4$) the denominator represents the total boron present in the system. The results shown in Fig. 4 confirm that all the Li$_2$O is indeed not utilized by B$_2$O$_3$ in the glass matrix as the observed values of N_4 are higher than that expected from PbO free lithium borate glasses in the $y/z > 1.0$ region. However as noted earlier, B$_3$ determined by NMR is, in reality, the sum of B$_3^0$ (BO$_{3/2}$), B$_2^-$ (BO$_{2/2}$O$^-$), and B$_1^{2-}$ (BO$_{1/2}$O$_2^{2-}$) species. PbO (P$_2^0$) reacts with B$_2^-$ in order to form P$_4^{2-}$ and B$_3^0$ without affecting the B$_3$ of NMR. But B$_4^-/$B$_3^0$ itself is affected significantly to manifest in the variation of the corresponding intensities in IR and Raman spectra. Also, since B$_3^0$ stabilizes B$_4^-$ very effectively. B$_4/$B$_3$ of NMR is also affected in a manner consistent with Fig. 4 ((B$_4/$B$_3$) is higher than that expected in the absence of PbO). In fact this is precisely what was expected from the equation which was used to justify the incorporation of PbO into the network. Since it has been seen from the IR and Raman spectra that Pb is likely to be present as [PbO$_{4/2}$]$^{2-}$ we assume tentatively that PbO is fully incorporated into the network reconverting B$_2^-$ and B$_1^{2-}$ species into B$_3^0$. For a given value of N_4, therefore, N_4z represents the number of moles of B$_2$O$_3$ present as B$_4$ units, where z is the mole fraction of B$_2$O$_3$. (N_4z)/2 of Li$_2$O has therefore been used for the formation of such B$_4$ units. Therefore ($y - (N_4z)/2$) of Li$_2$O (where y is the mole fraction of Li$_2$O) has in principle been available for conversion of PbO to [PbO$_{4/2}$]$^{2-}$. It is therefore possible that when ($y - (N_4z)/2$) is $> x$ (where x is the mole fraction

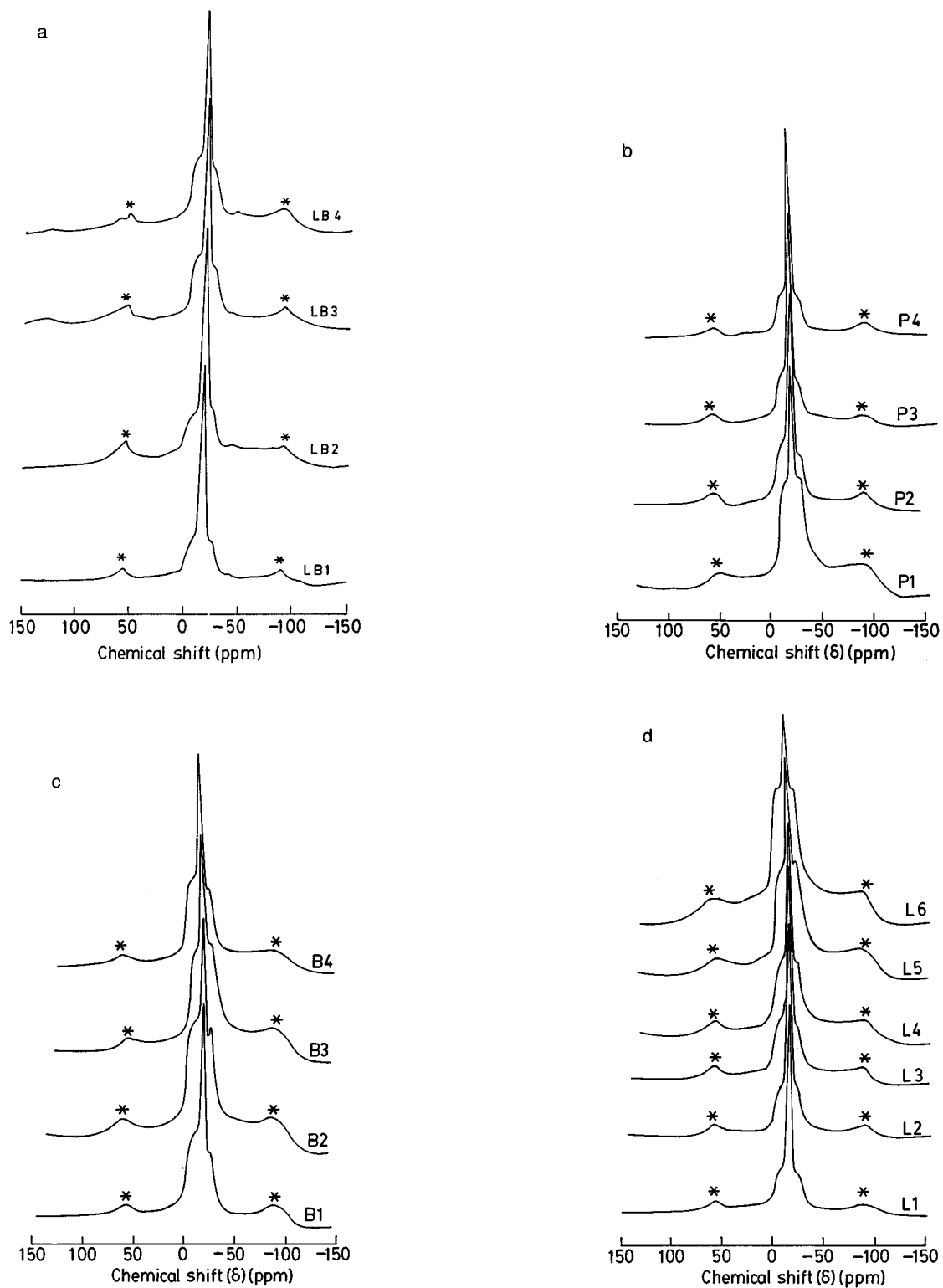**FIG. 3.** ^{11}B MASNMR spectra of (a) constant Li_2O/B_2O_3 (LB) series, (b) constant PbO (P) series, (c) constant B_2O_3 (B) series, and (d) constant Li_2O (L) series in the glass system $Li_2O–PbO–B_2O_3$. The spectra were recorded at a spinning speed of 7 KHz, the spinning sidebands are marked with *.

TABLE 4
Variation of N_4 with Composition in Li$_2$O–PbO–B$_2$O$_3$ Glasses as Determined from ^{11}B MASNMR Spectroscopy

Sample	N_4	x_{critical}^a
LB1	0.38	0.4
LB2	0.36	0.37
LB3	0.3	0.34
LB4	0.28	0.3
P1	0.12	0.48
P2	0.3	0.34
P3	0.4	0.2
P4	0.38	0.09
B1	0.22	0.67
B2	0.13	0.58
B3	0.12	0.48
B4	0.18	0.37
L1	0.38	0.4
L2	0.33	0.42
L3	0.3	0.44
L4	0.23	0.46
L5	0.12	0.48
L6	0.07	0.49

^{a} x_{critical} was calculated as $(y - (N_4 z)/2)$.

of PbO), all the PbO gets converted to $[\text{PbO}_{4/2}]^{2-}$. In those compositions where x_{critical}, i.e., $(y - (N_4 z)/2)$ is less than x, excess PbO remains in the structure. Then x is evidently dependent on the value of y and z. For example, x_{critical} is equal to 0.09 (Table 4) for P4 and it is less than the value of x (0.3) in the composition. We suggest that in this region of composition, PbO undergoes the following structural disproportionation
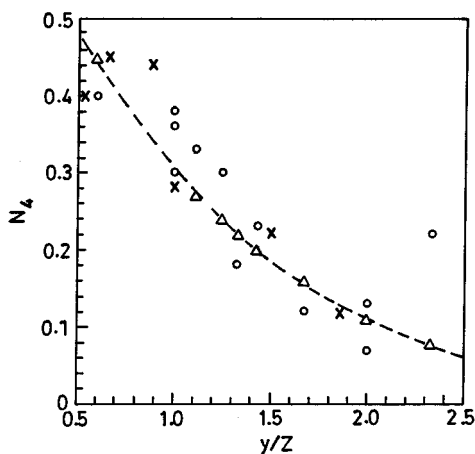
$$2\text{PbO} = [\text{PbO}_{4/2}]^{2-} + \text{Pb}^{2+}.$$

FIG. 4. Variation of N_4 with y/z. ○ denotes the experimental N_4 values determined by NMR, x denotes some experimental N_4 values for the binary Li$_2$O–B$_2$O$_3$ glasses. The dotted line represents the variation of the empirical function $1/2\exp(1/2 - y/z)$ with y/z.

A similar structural disproportionation is known to occur in the case of Al in aluminosilicates where part of the aluminum is present in tetrahedral network positions and part as Al^{3+} ions coordinated to a larger number of oxygens (53). In fact $(y - (N_4 z)/2) > x$ in most of the glasses except for P3 and P4 where a structural disproportionation of PbO may occur. Therefore, the present investigation strongly points toward a tendency of PbO to become incorporated into the network.

CONCLUSIONS

Characterization of a number of glasses in the pseudoternary glass system Li$_2$O–PbO–B$_2$O$_3$ seems to indicate the network forming role of PbO in these glasses. It is likely that PbO is incorporated in the network as $[\text{PbO}_{4/2}]^{2-}$ and in the process results in the creation of three-coordinated boron (B$_3^0$) and four coordinated boron (B$_4^-$) at the expense of two- and one-coordinated boron (B$_2^-$ and B$_1^{2-}$, respectively). IR and Raman spectroscopic features support this conjecture. The N_4 values determined from ^{11}B MASNMR indicate that the B$_4$/B$_3$ ratio is higher than that expected in PbO free borates and is consistent with the suggestion that PbO is incorporated into the network. Variation of glass transition temperatures and molar volumes with composition also support the structural model proposed for these glasses.

ACKNOWLEDGMENTS

REFERENCES

1. A. R. Kulkarni, H.S. Maiti, and A. Paul *Bull. Mater. Sci.* **6,** 201 (1984).
2. B. V. R. Chowdhari and S. Radhakrishna, "Materials for Solid State Batteries." World Scientific, Singapore, 1986.
3. M. D. Ingram, *Phys. Chem. Glasses* **28,** 215 (1987).
4. C. A. Angell, *Chem. Rev.* **90,** 523 (1990).
5. C. A. Angell, *Ann. Rev. Phys. Chem.* **43,** 693 (1992).
6. K. J. Rao and M. Ganguli *in* "Handbook of Solid State Batteries and Capacitors" (M. A. Z. Munshi, Ed.), p. 189. World Scientific, Singapore, 1995.
7. L. D. Pye, V. D. Frechette, and N. J. Kreidel, "Borate Glasses: Structure, Properties and Applications." Plenum Press, New York, 1978.
8. R. Rawson, "Inorganic Glass Forming Systems." Academic Press, London, 1967.
9. J. Krogh-Moe, *Phys. Chem. Glasses* **1,** 26 (1960).
10. J. Krogh-Moe, *Phys. Chem. Glasses* **3,** 101, 208 (1962).
11. J. Krogh-Moe, *Phys. Chem. Glasses* **6,** 46 (1965).
12. W. L. Konijnendijk and J. M. Stevels, *J. Non-Cryst. Solids* **18,** 307 (1975).
13. W. L. Konijnendijk, *Philips Res. Rep. Suppl.* **1,** 243 (1975).

14. D. L. Griscom *in* "Borate Glasses: Structure, Properties and Applications" (L. D. Pye, V. D. Frechette, and N. J. Kreidel, Eds.), Plenum Press, New York, 1978.
15. P. J. Bray and J. G. O'Keefe, *Phys. Chem. Glasses* **4,** 37 (1963).
16. E. I. Kamitsos, M. A. Karakassides, and G.D. Chryssikos, *Phys. Chem. Glasses* **30,** 229 (1989).
17. G. D. Chryssikos, E.I. Kamitsos, and M. A. Karakassides, *Phys. Chem. Glasses* **31,** 109 (1990).
18. A. H. Silver and P. J. Bray, *J. Chem. Phys.* **19,** 984 (1958).
19. U. Selvaraj and K. J. Rao, *Spectrochim. Acta A*, **40,** 1081 (1984).
20. P. J. Bray, M. Leventhal, and H. O. Hooper, *Phys. Chem. Glasses* **4,** 47 (1963).
21. M. Leventhal, and P. J. Bray, *Phys. Chem. Glasses* **6,** 113 (1965).
22. B. N. Meera, A. K. Sood, N. Chandrabhas, and J. Ramakrishna, *J. Non-Cryst. Solids* **126,** 224 (1990).
23. B. Wang, S. P. Szu, and M. Greenblatt, *J. Non-Cryst. Solids* **134,** 249 (1991).
24. B.G. Rao, H. G. K. Sundar, and K. J. Rao, *J. Chem. Soc. Faraday Trans. 1* **80,** 3491 (1984).
25. K. J. Rao, B. G. Rao, and S.R. Elliott, *J. Mater. Sci.* **20,** 1678 (1985).
26. A. M. Zahra and C. Y. Zahra, *J. Non-Cryst. Solids* **155,** 45 (1993).
27. J. Lorosch, M. Couzi, J. Petous, R. Vacher, and A. Levasseur, *J. Non-Cryst. Solids* **69,** 1 (1984).
28. K. Witke, M. Willfahrt, TH. Hubert, and P. Reich, *J. Molec. Struct.* **349,** 373 (1995).
29. U. Selvaraj and K. J. Rao, *J. Non-Cryst. Solids* **104,** 300 (1988).
30. S. R. Elliott, "Physics of Amorphous Materials." Longman, London, 1984.
31. E. I. Kamitsos, M. A. Karakassides, and G. D. Chryssikos, *Phys. Chem. Glasses* **28,** 203 (1987).
32. E. I. Kamitsos, M. A. Karakassides, and G. D. Chryssikos, *J. Phys. Chem.* **91,** 1073 (1987).
33. E. I. Kamitsos, A. P. Patsis, M. A. Karakassides, and G. D. Chryssikos, *J. Non-Cryst. Solids* **126,** 52 (1990).
34. D. N. Sathyanarayana, "Vibrational Spectroscopy: Theory and Applications." New Age International, New Delhi, 1996.
35. J. Zhong and P. J. Bray, *J. Non-Cryst. Solids* **111,** 67 (1989).
36. R. T. Sanderson, "Polar Covalence." Academic Press, New York, 1983.
37. S. Muthupari and K. J. Rao, *J. Phys. Chem.* **98,** 2646 (1994).
38. E. I. Kamitsos, and M. A. Karakassides, *Phys. Chem. Glasses* **30,** 19 (1989).
39. E. I. Kamitsos, M. A. Karakassides, and A. P. Patsis, *J. Non-Cryst. Solids* **111,** 252 (1989).
40. G. D. Chryssikos, E. I. Kamitsos, A. P. Patsis, and M. A. Karakassides, *Mater. Sci. Eng. B* **7,** 1 (1990).
41. B. N. Meera and J. Ramakrishna, *J. Non-Cryst. Solids* **159,** 1 (1993).
42. J. Wong and C. A. Angell, "Glass Structure by Spectroscopy." Marcel Dekker, New York, 1976.
43. P. Tarte, *Spectrochim. Acta* **20,** 238 (1964).
44. M. Ganguli and K. J. Rao, *J. Non-Cryst. Solids* **243,** 251 (1999).
45. K. B. Dillon and T. C. Waddington, *Spectrochim. Acta A* **30,** 1873 (1974).
46. S. Prabhakar, K. J. Rao, and C. N. R. Rao, *Proc. Royal Soc.* (*London*) *A* **429,** 1 (1990).
47. S. Greenblatt and P. J. Bray, *Phys. Chem. Glasses* **8,** 213 (1967).
48. G. E. Jellison Jr. and P. J. Bray, *J. Non-Cryst. Solids* **29,** 187 (1978).
49. C. A. Fyfe, "Solid State NMR for Chemists." CNC Press, Guelph, 1983.
50. P. J. Bray, *J. Non-Cryst. Solids* **75,** 29 (1985).
51. Y. H. Yun and P. J. Bray, *J. Non-Cryst. Solids* **44,** 227 (1981).
52. M. Ganguli and K. J. Rao, *J. Phys. Chem.* **103,** 920 (1999).
53. S. Prabhakar, K. J. Rao, and C. N. R. Rao, *Eur. J. Solid State Inorg. Chem.* **29,** 95 (1992).